Progress In Electromagnetics Research, PIER 79, 195–208, 2008

A CLOSED-FORM SOLUTION TO ANALYZE RCS OF CAVITY WITH RECTANGULAR CROSS SECTION

L. Xu, J. Tian, and X. W. Shi

National Key Laboratory of Antenna and Microwave Technology
Xidian University
NO. 2 SOUTH Taibai ROAD Xi'an, Shaanxi, P. R. China

Abstract—In this paper, a set of formulas to analyze the scattering from open-ended rectangular cavity is presented on the basis of Shooting and Bouncing Ray (SBR) method. By analyzing the ray paths inside the cavity, the Physical-Optics (PO) integration on the aperture is carried out in a close form. Using closed-form solution, the Radar Cross Section (RCS) of cavity in high frequency can be studied sententiously and accurately. All the peaks and nulls in the RCS plot of cavity are predicted successfully with the formulas deduced in the paper, and a 3-D scattering pattern of rectangular cavity is simulated by the proposed method.

1. INTRODUCTION

The problem of electromagnetic scattering from open-ended cavities has been studied intensively by various computational electromagnetic techniques for many years [1–5]. This problem serves as a simple model of duct structures such as Jet engine intakes or antenna windows embedded in more complex bodies [1, 6–8], and much research has been carried out on analysis of both radar cross section and electromagnetic pulse coupling [9–12]. At the low frequency end, i.e., cavities with opening less than a wave-length, a rigorous integral equation can be used [1, 5]. For an aperture opening on the order of several wavelengths, one has to resort to high-frequency approximations [4].

The shooting and bouncing ray (SBR) method is proposed to study the scattering from cavity for decades [3, 4, 9], and it has been widely used in the simulation of electromagnetic wave scattering from cavity. The validity and accuracy of SBR method is proved in many papers available. In order to analyze the scattering from cavity upon complex object, some hybrid methods of SBR with other computational electromagnetic techniques are developed. The SBR method is know as a powerful RCS analysis method because it can analyze the RCS characteristics for arbitrary shape open-ended cavities, and it is also widely used if the space inside the cavity is not homogeneous or the electrical dimension of the cavity is large [3]. While much research has been devoted to the problem that shape of the cavity is arbitrary, little research has been done on the acceleration of SBR method to analyze the cavity in large size.

Owning to the irregular positions of exit rays, the physical-optics integration cannot be easily carried out in original SBR [3]. Although the SBR approach can predict RCS for cavity in any shape, it is time-consuming and unpractical to realize modeling of the physical problems for cavity in large size. There are also other methods that can be used to calculate the scattering from cavity, such as waveguide modal approach, but it is cumbersome if the electrical dimension of the cavity is very large.

The present paper discusses the characteristics of ray tracing inside the cavity with typical shape such as rectangular cross section, which is applied widely in the fields of electromagnetic. A closed-form solution for analysis the RCS of rectangular cavity is developed based on the SBR method. The formulas are of concise expression and can be realized easily by computer. The characteristic of rectangular cavity is studied, such as the peaks and nulls in the RCS plot of cavity, and the scattering pattern for rectangular cavity is presented, which is difficult to be realized by the original SBR or other methods.

2. PREDICTION METHOD

In the SBR method, the incident wave is divided into a set of ray tubes. By the approach of ray tracing and physical optics integral, the scattering from cavity is calculated. A detailed procedure of the SBR can be found in [3]. On the basis of a study on ray tracing, the positions of ray bounced on the wall of cavity and the location of ray exit are analyzed, and the rules of ray path inside the cavity are investigated. The property of ray bouncing in rectangular cavity is discussed in this paper, and the relation between ray incident and ray exit is deduced. A closed-form solution for 3-D problems of scattering from rectangular cavity is presented. The procedure is bored and complex, and some important results are listed here.

The backscattered field can be carried out by the follows [3]:

$$\vec{E} = \frac{e^{-jk_0 r}}{r}[\hat{\theta}A_\theta + \hat{\varphi}A_\varphi]$$
$$\begin{bmatrix} A_\theta \\ A_\varphi \end{bmatrix} = \frac{jk_0}{2\pi}\sum_m \begin{bmatrix} E_{xm}\cos\varphi^i + E_{ym}\sin\varphi^i \\ -(E_{xm}\sin\varphi^i + E_{ym}\cos\varphi^i)\cos\theta^i \end{bmatrix} I_m e^{jk_0\hat{s}_m\cdot\vec{r}_m} \tag{1}$$

Here, I_m is defined as follows,

$$I_m = \iint\limits_{\substack{mth\ exit \\ ray\ tube}} dxdye^{-jk_0(\hat{i}_m+\hat{s}_m)\cdot\vec{r}} \tag{2}$$

In Eq. (1), m is the index of ray tube. E_{xm} and E_{ym} are the x and y components of the outgoing field on the aperture. The direction vectors of the incident rays and exit rays for mth ray tube are denoted by $\hat{i}_m$ and $\hat{s}_m$ respectively, and the central ray in mth exit ray tube hits aperture of cavity at point $\vec{r}_m = (x_m, y_m)$.

Eq. (2) is the Fourier transform of the ray tube shape function (normalized with respect to the ray tube area), and it can be carried out as follows:

$$\begin{aligned} I_m = &(\Delta x_m \Delta y_m)e^{-jk_0(\hat{i}_m+\hat{s}_m)\cdot\vec{r}_m} \\ &\times sha\left[k_0(i_{mx}+s_{mx})\frac{\Delta x_m}{2}\right] sha\left[k_0(i_{my}+s_{my})\frac{\Delta y_m}{2}\right] \end{aligned} \tag{3}$$

Where,

$$sha(x) = \frac{\sin x}{x}$$
$$(\Delta x_m \Delta y_m) = area\ of\ the\ exit\ ray\ tube.$$

In order to get a precise result, the dimension of ray tube is supposed to tend to zero, and Eq. (3) can be carried out with a new expression:

$$I_m = (\Delta x_m \Delta y_m)e^{-jk_0(\hat{i}_m+\hat{s}_m)\cdot\vec{r}_m} \tag{4}$$

The geometry of rectangular cavity is shown in Fig. 1, and Fig. 2 is the local coordinate system at the reflected point on the wall of cavity.

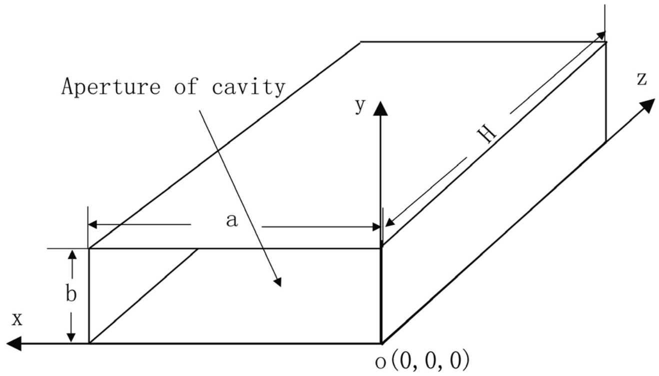

Figure 1. Geometry for rectangular cavity.

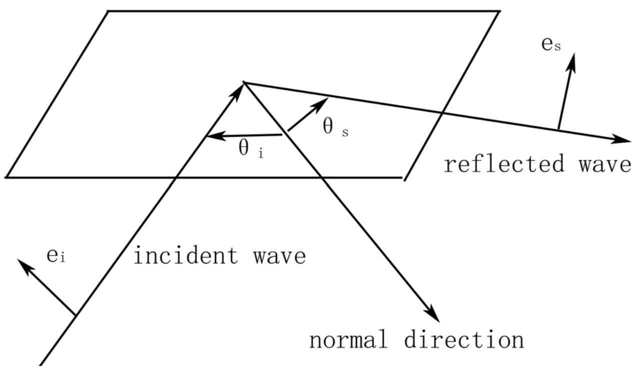

Figure 2. Local coordinate system at reflect point.

According to the reflection laws of plane wave incidence on a dielectric interface, some special rules for ray bounced in rectangular cavity can be found:

$$\left\{\begin{array}{l}\hat{i}=(\sin\theta^i\cos\varphi^i,\sin\theta^i\sin\varphi^i,\cos\theta^i)\\ \hat{s}=\hat{i}-2(\hat{i}\cdot\hat{n})\hat{n}\end{array}\right. \tag{5}$$

$$\hat{e}^s=2(\hat{e}^i\cdot\hat{n})\hat{n}-\Gamma_{//}\hat{e}^i_{//}+\Gamma_{\perp}\hat{e}^i_{\perp} \tag{6}$$

Where, $\hat{i}$, $\hat{s}$, $\hat{e}^i$ and $\hat{e}^s$ are the direction vectors of the incident wave, reflected wave, incident electric field and reflected electric field respectively. The subscript $\|$ and $\perp$ represent the components of parallel or perpendicular polarization accordingly. If the wall of cavity is perfect conductor, then Eq. (6) can be rewritten into:

$$\hat{e}^s = 2(\hat{e}^i \cdot \hat{n})\hat{n} - \hat{e}^i \tag{7}$$

Consider one of the incident ray tubes, given the location of incident ray hit on the aperture, a set of reflected points in cavity and the direction of the exiting ray can be obtained with the Geometric Optics (GO) method. The detailed process of ray tracing is bored and lengthy so only some results are described here.

In order to carry out Eq. (1), the relationship of incident ray tube and exit ray tube should be determined at firstly. Given the incident field, the ray paths in the cavity can be found by ray tracing and the rules proposed above, and the field amplitude of the exit rays on the aperture of cavity is got based on GO method. Table 1 presents a summarization of the relation between incident ray and ray exit. As

Table 1. Relationship of ray incident and ray exit on the aperture.

<table>
<tr><td rowspan="2">N_{0x} is odd</td><td>$x \in [0, B_x]$</td><td>$x_{out} = x + a - B_x$</td><td>$s_x = i_x$</td><td>$e_y^s = e_y^i$
$e_z^s = e_z^i$</td><td rowspan="4">e_x^s $\|$ $-e_x^i$</td><td rowspan="8">s_z $\|$ $-i_z$</td></tr>
<tr><td>$x \in [B_x$,a]</td><td>$x_{out} = -x+a+B_x$</td><td>$s_x = -i_x$</td><td>$e_y^s = -e_y^i$
$e_z^s = -e_z^i$</td></tr>
<tr><td rowspan="2">N_{0x} is even</td><td>$x \in [0, B_x]$</td><td>$x_{out} = -x + B_x$</td><td>$s_x = -i_x$</td><td>$e_y^s = -e_y^i$
$e_z^s = -e_z^i$</td></tr>
<tr><td>$x \in [B_x$,a]</td><td>$x_{out} = x - B_x$</td><td>$s_x = i_x$</td><td>$e_y^s = e_y^i$
$e_z^s = e_z^i$</td></tr>
<tr><td rowspan="2">N_{0y} is odd</td><td>$y \in [0, B_y]$</td><td>$y_{out} = y + b - B_y$</td><td>$s_y = i_y$</td><td>$e_x^s = e_x^i$
$e_z^s = e_z^i$</td><td rowspan="4">e_y^s $\|$ $-e_y^i$</td></tr>
<tr><td>$y \in [B_y$,b]</td><td>$y_{out} = -y+b+B_y$</td><td>$s_y = -i_y$</td><td>$e_x^s = -e_x^i$
$e_z^s = -e_z^i$</td></tr>
<tr><td rowspan="2">N_{0y} is even</td><td>$y \in [0, B_y]$</td><td>$y_{out} = -y + B_y$</td><td>$s_y = -i_y$</td><td>$e_x^s = -e_x^i$
$e_z^s = -e_z^i$</td></tr>
<tr><td>$y \in [B_y$,b]</td><td>$y_{out} = y - B_y$</td><td>$s_y = i_y$</td><td>$e_x^s = e_x^i$
$e_z^s = e_z^i$</td></tr>
</table>

the axis of cavity is parallel to the Z axis in Cartesian coordinates, the location of ray incident and ray exit can be represented by (x, y) and (x_{out}, y_{out}) respectively. The parameters N_{0x}, N_{0y}, B_x and B_y in Table 1 are defined as follows:

$$N_{0x} = Round\left(\frac{2h}{a} \cdot \frac{|i_x|}{i_z}\right) + 1 \tag{8}$$

$$N_{0y} = Round\left(\frac{2h}{b}\cdot\frac{|i_y|}{i_z}\right)+1 \tag{9}$$

$$B_x = \left(N_{0x}a - \frac{|i_x|}{i_z}2h\right) \tag{10}$$

$$B_y = \left(N_{0y}b - \frac{|i_y|}{i_z}2h\right) \tag{11}$$

Once the incident rays have been defined, the impact point of each ray on the inner wall or the bottom of the cavity will be determined, and the parameters N_{0x}, N_{0y}, B_x and B_y can be carried out, which will confirm the exit ray by the relationship shown in Table 1. For example, consider the case in which N_{0x} is odd and N_{0y} is even, while incident ray hits the aperture of cavity at point (x, y), if $x \in [0, B_x]$ and $y \in [0, B_y]$, then then exit ray can be confirmed as following equations:

$$\begin{cases} x_{out} = x + a - B_x \\ y_{out} = -y + B_y \\ \hat{s} = (i_x, -i_y, -i_z) \\ \hat{e}^s = (e_x^i, -e_y^i, -e_z^i) \end{cases}$$

As mentioned above, there should be enough ray tubes launched into cavity to get an accurate result in SBR method, and the sizes of ray tube must tend to zero ($\Delta x \to 0$, $\Delta y \to 0$), which means that the sum in Eq. (1) can be replaced by an integral operation, so Eq. (1) is rewritten as:

$$\begin{bmatrix} A_\theta \\ A_\varphi \end{bmatrix} = \frac{jk_0}{2\pi}e^{-jk_0\frac{2h}{i_z}}\iint\limits_S \begin{bmatrix} E_{outx}\cos\varphi^i + E_{outy}\sin\varphi^i \\ -(E_{outx}\sin\varphi^i + E_{outy}\cos\varphi^i)\cos\theta^i \end{bmatrix} \times e^{-jk_0\hat{i}\cdot(\vec{r}_{out}-\vec{r})}dx_{out}dy_{out} \tag{12}$$

Where, subscript *out* means the components related to ray exit. Because the positions of exit rays are nonuniformly dispersed over the aperture, the integration in Eq. (12) cannot be carried out directly. However, the incident rays are launched uniformly. If we can carry out Eq. (12) with the incident field on the aperture instead of outgoing field, the integration may be solved out. As seen from Table 1, the relation between $\vec{r} = (x, y)$ and $\vec{r}_{out} = (x_{out}, y_{out})$ can be concluded as follows,

$$\begin{aligned} x &= \pm x_{out} + C1 \\ y &= \pm y_{out} + C2 \end{aligned} \tag{13}$$

Where, $C1$ and $C2$ are constant corresponding. That is to say, $dx_{out}dy_{out}$ can be replaced by $\pm dxdy$, which implies that the integral region may be converted to the aperture of cavity. The sign $\pm$ will be determined by the relationship of incident ray and exit ray, which is shown in Table 1. In order to get a closed-form solution of Eq. (12), the aperture of cavity is divided into four subregions which are shown in Fig. 3.

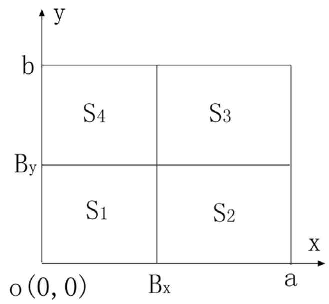

Figure 3. Subregions of integral region.

As an example, the paper carries out the integral in Eq. (12) when $N_{0x}$and N_{0y} are both odd. The solution for other cases can be deduced in a similar procedure, and the paper doesn't list them here. Let the integral part of Eq. (12) on region S_1 be denoted by I_{s1}, then:

$$\begin{aligned} I_{s1} &= \iint\limits_{S1} \begin{bmatrix} -e_x^i \cos\varphi^i - e_y^i \sin\varphi^i \\ (e_x^i \sin\varphi^i - e_y^i \cos\varphi^i)\cos\theta^i \end{bmatrix} e^{-jk_0(i_x x + i_y y)} \\ &\quad \times e^{-jk_0[i_x(x+a-B_x)+i_y(y+b-B_y)]} dxdy \\ &= \begin{bmatrix} -e_x^i \cos\varphi^i - e_y^i \sin\varphi^i \\ (e_x^i \sin\varphi^i - e_y^i \cos\varphi^i)\cos\theta^i \end{bmatrix} e^{-jk_0(i_x a + i_y b)} \\ &\quad \times B_x B_y sha(k_0 i_x B_x) sha(k_0 i_y B_y) \end{aligned} \tag{14}$$

$$\begin{aligned} I_{s2} &= -\begin{bmatrix} -e_x^i \cos\varphi^i + e_y^i \sin\varphi^i \\ (e_x^i \sin\varphi^i + e_y^i \cos\varphi^i)\cos\theta^i \end{bmatrix} e^{-jk_0[i_x(a+B_x)+i_y b]} \\ &\quad \times (a-B_x) B_y sha(k_0 i_y B_y) \end{aligned} \tag{15}$$

$$\begin{aligned} I_{s3} &= \begin{bmatrix} e_x^i \cos\varphi^i + e_y^i \sin\varphi^i \\ (-e_x^i \sin\varphi^i + e_y^i \cos\varphi^i)\cos\theta^i \end{bmatrix} e^{-jk_0[i_x(a+B_x)+i_y(b+B_y)]} \\ &\quad \times (a-B_x)(b-B_y) \end{aligned} \tag{16}$$

$$I_{s4} = -\begin{bmatrix} e_x^i \cos\varphi^i - e_y^i \sin\varphi^i \\ (-e_x^i \sin\varphi^i - e_y^i \cos\varphi^i)\cos\theta^i \end{bmatrix} e^{-jk_0[i_x a + i_y(b+B_y)]} \times B_x(b-B_y) sha(k_0 i_x B_x) \tag{17}$$

Obviously, the integral in Eq. (12) is the sum of four integrals in those subregions. Once the integral is carried out, Eq. (12) is solved in a closed-form.

The formulas for other case are list as follows.

1). If N_{0x} is odd and N_{0y} is even,

$$I_{s1} = -\begin{bmatrix} e_x^i \cos\varphi^i - e_y^i \sin\varphi^i \\ (-e_x^i \sin\varphi^i - e_y^i \cos\varphi^i)\cos\theta^i \end{bmatrix} e^{-jk_0(i_x a + i_y B_y)} \times B_x B_y sha(k_0 i_x B_x) \tag{18}$$

$$I_{s2} = \begin{bmatrix} e_x^i \cos\varphi^i + e_y^i \sin\varphi^i \\ (-e_x^i \sin\varphi^i + e_y^i \cos\varphi^i)\cos\theta^i \end{bmatrix} e^{-jk_0[i_x(a+B_x) + i_y B_y]} \times (a-B_x) B_y \tag{19}$$

$$I_{s3} = -\begin{bmatrix} -e_x^i \cos\varphi^i + e_y^i \sin\varphi^i \\ (e_x^i \sin\varphi^i + e_y^i \cos\varphi^i)\cos\theta^i \end{bmatrix} e^{-jk_0[i_x(a+B_x) + i_y b]} \times (a-B_x)(b-B_y) sha[k_0 i_y(b-B_y)] \tag{20}$$

$$I_{s4} = \begin{bmatrix} -e_x^i \cos\varphi^i - e_y^i \sin\varphi^i \\ (e_x^i \sin\varphi^i - e_y^i \cos\varphi^i)\cos\theta^i \end{bmatrix} e^{-jk_0(i_x a + i_y b)} \times B_x(b-B_y) sha(k_0 i_x B_x) sha[k_0 i_y(b-B_y)] \tag{21}$$

2). If N_{0x} is even and N_{0y} is odd,

$$I_{s1} = -\begin{bmatrix} -e_x^i \cos\varphi^i + e_y^i \sin\varphi^i \\ (e_x^i \sin\varphi^i + e_y^i \cos\varphi^i)\cos\theta^i \end{bmatrix} e^{-jk_0(i_x B_x + i_y b)} \times B_x B_y sha(k_0 i_y B_y) \tag{22}$$

$$I_{s2} = \begin{bmatrix} -e_x^i \cos\varphi^i - e_y^i \sin\varphi^i \\ (e_x^i \sin\varphi^i - e_y^i \cos\varphi^i)\cos\theta^i \end{bmatrix} e^{-jk_0(i_x a + i_y b)} \times (a-B_x) B_y sha[k_0 i_x(a-B_x)] sha(k_0 i_y B_y) \tag{23}$$

$$I_{s3} = -\begin{bmatrix} e_x^i \cos\varphi^i - e_y^i \sin\varphi^i \\ (-e_x^i \sin\varphi^i - e_y^i \cos\varphi^i)\cos\theta^i \end{bmatrix} e^{-jk_0[i_x a + i_y(b+B_y)]} \times (a-B_x)(b-B_y) sha[k_0 i_x (a-B_x)] \tag{24}$$

$$I_{s4} = \begin{bmatrix} e_x^i \cos\varphi^i + e_y^i \sin\varphi^i \\ (-e_x^i \sin\varphi^i + e_y^i \cos\varphi^i)\cos\theta^i \end{bmatrix} e^{-jk_0[i_x B_x + i_y(b+B_y)]} \times B_x(b-B_y) \tag{25}$$

3). If N_{0x} is even and N_{0y} is even,

$$I_{s1} = \begin{bmatrix} e_x^i \cos\varphi^i + e_y^i \sin\varphi^i \\ (-e_x^i \sin\varphi^i + e_y^i \cos\varphi^i)\cos\theta^i \end{bmatrix} e^{-jk_0(i_x B_x + i_y B_y)} B_x B_y \tag{26}$$

$$I_{s2} = -\begin{bmatrix} e_x^i \cos\varphi^i - e_y^i \sin\varphi^i \\ (-e_x^i \sin\varphi^i - e_y^i \cos\varphi^i)\cos\theta^i \end{bmatrix} e^{-jk_0(i_x a + i_y B_y)} \times (a-B_x) B_y sha[k_0 i_x (a-B_x)] \tag{27}$$

$$I_{s3} = \begin{bmatrix} -e_x^i \cos\varphi^i - e_y^i \sin\varphi^i \\ (e_x^i \sin\varphi^i - e_y^i \cos\varphi^i)\cos\theta^i \end{bmatrix} e^{-jk_0(i_x a + i_y b)} \times (a-B_x)(b-B_y) sha[k_0 i_x (a-B_x)] sha[k_0 i_y (b-B_y)] \tag{28}$$

$$I_{s4} = -\begin{bmatrix} -e_x^i \cos\varphi^i + e_y^i \sin\varphi^i \\ (e_x^i \sin\varphi^i + e_y^i \cos\varphi^i)\cos\theta^i \end{bmatrix} e^{-jk_0(i_x B_x + i_y b)} \times B_x(b-B_y) sha[k_0 i_y (b-B_y)] \tag{29}$$

Then, Eq. (12) can be carried out in a close form as shown below.

$$\begin{bmatrix} A_\theta \\ A_\varphi \end{bmatrix} = \frac{jk_0}{2\pi} e^{-jk_0 \frac{2h}{i_z}} \times I \tag{30}$$

where,

$$I = I_{s1} + I_{s2} + I_{s3} + I_{s4}$$

The proposed method is summarized below,

1) Input the geometry size of cavity ($a \times b \times H$) and the direction of incident wave $\hat{i}$;
2) Calculate the values of N_{0x}, N_{0y}, B_x and B_y by the equations Eqs. (8)–(11);

3) Select a set of integral formulas according to whether N_{0x} and N_{0y} are odd or even;
4) Carry out Eq. (30) with the integrals solved by step 3.

With the closed-form solution based on SBR method, the scattering from rectangular cavity can be simulated succinctly. Without worrying about time-consuming, the method is able to deal with the problems in high frequency.

3. RESULTS AND ANALYSIS

As the validity of SBR method is tested in many papers available [3, 4], and the purpose of the paper was to provide a method to analyze the electromagnetic scattering from rectangular cavity in high precision and fast speed, so the objective of the present simulations was to verify the validity of new method and investigate the characteristics of rectangular cavity. The scattering pattern of rectangular cavity is visualized to show the advantage of proposed method.

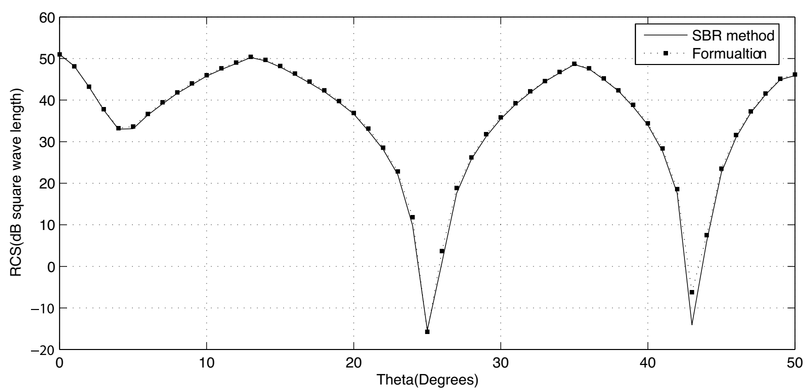

Figure 4. Comparison between the results traditional SBR method and formulation, $\varphi = 45^o$

Firstly, the results in traditional SBR and closed-form formulas are compared in Fig. 4 to verify the correctness of the developed method. The example is selected from the literature [4], which studied a rectangular cavity with a 10λ by 10λ square cross section and 30λ in length. Excellent agreements can be found between two curves. The results show an interesting phenomenon that almost all nulls and peaks in curve take place where the value of $\frac{2h}{a} \cdot \frac{|i_x|}{i_z}$ is an integer. Referring to the closed-form expression, it can be explained visually. In Eq. (8), B_x

tends to zero as $\frac{2h}{a} \cdot \frac{|i_x|}{i_z}$ is close to an integer number. That is to say, according to Table 1, nearly all ray tubes exit cavity in the direction of incident wave or in the contrary direction. It can be predicted exactly that peaks will take place at $\theta^i = 13.26°$, $35.26°$ and so on, when the ray exit cavity in the direction of incident ray. There will be a null at $\theta^i = 25.24°$, $43.31°$ when ray exit cavity in a contrary direction.

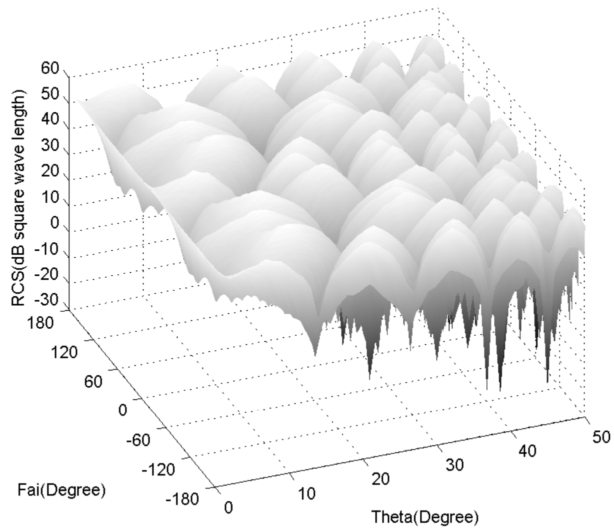

Figure 5. Pattern of $RCS_{\theta\theta}$ for rectangular cavity.

Then, a pattern of scattering from cavity is shown in Fig. 5. Benefited from the solution in closed-form, simulation of RCS pattern in 3-D becomes practicable. In order to avoid some special phenomena for cavity with square cross section, a rectangular cavity with dimensions $a = 10\lambda$, $b = 15\lambda$ and $H = 40\lambda$ is selected, and the paper calculates the RCS in parallel polarization. As complicated procedure of ray tracing in SBR method, pattern analysis of cavity is a burdensome work for traditional SBR. With the closed-form formulas proposed here, it takes few seconds to get the results. Fig. 6 shows the projection of pattern to the x-o-y plane. Due to the symmetry of geometry, the image shows symmetrical characteristic with the variation of φ^i. As mentioned above, it can be predicted that there are four nulls at $\varphi^i = 0°$ and three nulls at $\varphi^i = 90°$. Fig. 6 shows that the size of cavity in width plays an important role in the region from $\varphi^i = -16°$ to $\varphi^i = 16°$, and the size of cavity in height is important in the region from $\varphi^i = -78°$ to $\varphi^i = -100°$. The impact of geometry size on scattering characters of cavity can be studied in

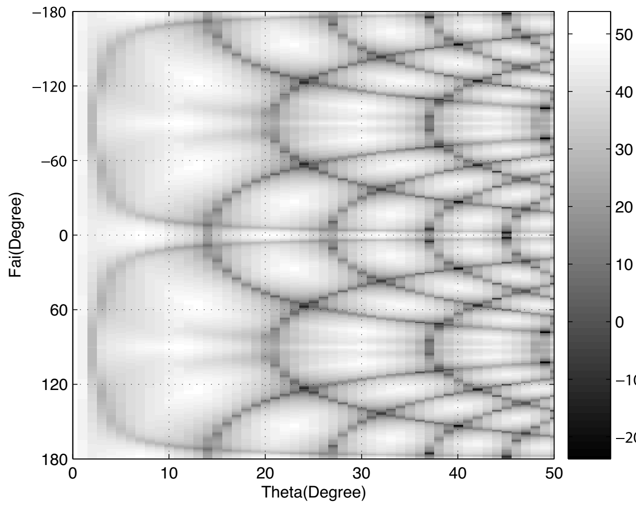

Figure 6. Projection of $RCS_{\theta\theta}$ pattern to X-O-Y plane.

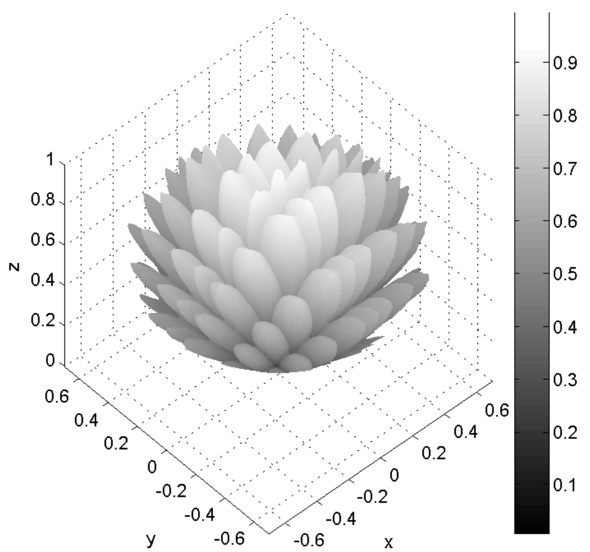

Figure 7. Pattern of $RCS_{\theta\theta}$ for rectangular cavity in sphere coordinates.

detail with equations from Eq. (8) to Eq. (11). In order to give a visual understanding of RCS pattern for cavity, Fig. 7 plots the normalized RCS pattern in sphere coordinates.

4. CONCLUSIONS

A set of formulas was proposed to calculate the electromagnetic scattering from a rectangular cavity. This approach is based on the SBR method by taking into consideration 1) launching enough ray tubes into the cavity, 2) tracking the ray path inside the cavity, and 3) determining the GO field associated with each incident ray. The relation between incident rays and exit rays is found by investigating the characteristics of ray launched into the cavity. The sum of the scattered field due to each individual exit ray tube is replaced by an integral of incident rays on aperture of cavity, and a 3-D closed-form solution based on SBR to analyze the high frequency backscattering from open cavities are carried out. Although there are other analytical solutions that may be possible for regular shapes, they become cumbersome if the electrical dimension of the cavity is large. Using the proposed method, the problem of cavity with rectangular cross section can be solved in high speed and precision, and it makes scattering pattern simulation for cavity possible. The locations of peaks and nulls in the scattering are predicted accurately with the formulas proposed in the paper. The scattering pattern of rectangular cavity is visualized by the closed-form formulas, and some interesting characteristic is presented. Due to the assumption that the size of ray tube in SBR tends to infinitesimal, a higher precision of results is expected.

REFERENCES

1. Huddleston, P., "Scattering from conducting finite cylinders with thin coatings," *IEEE Trans. Antennas Propagat.*, Vol. 43, 1128–1136, 1987.
2. Altintas, A., P. H. Pathak, and M. C. Liang, "A selective modal scheme for the analysis of EM coupling into orradiation from large open-ended waveguides," *IEEE Trans. Antennas Propagat.*, Vol. 36, 84–96, 1988.
3. Ling, H., R. C. Chou, and S. W. Lee, "Shooting and bouncing rays: calculating the RCS of an arbitrarily shaped cavity," *IEEE Trans. Antennas Propagat.*, Vol. 47, 961–969, 1999.

4. Ling, H., S. W. Lee, and R. C.Chou, "High-frequency RCS of open cavities with rectangular and circular cross sections," *IEEE Trans. Antennas Propagat.*, Vol. 37, 648–654, 1989.
5. Medgyesi, M. L. and C. Eftimiu, "Scattering from wires and open circular cylinders of finite length using entire domain Galerkin expansions," *IEEE Trans. Antennas Propagat.*, Vol. 30, 628–636, 1982.
6. Bopp, C. L. and C. M. Butler, "Analysis of transmission of a signal through a complex cylindrical/coaxial cavity by transmission line methods," *Progress In Electromagnetics Research*, PIER 56, 33–51, 2006.
7. Nie, X. C., Y. B. Gan, N. Yuan, et al., "An efficient hybrid method for analysis of slot arrays enclosed by a large radome," *Journal of Electromagnetic Waves and Applications*, Vol. 20, 249–264, 2006.
8. Li, J. Y., L. W. Li, and Y. B. Gan, "Method of moments analysis of waveguide slot antennas using the EFIE," *Journal of Electromagnetic Waves and Applications*, Vol. 19, 1729–1748, 2005.
9. Chen, C. H., C. L. Liu, C. C. Chiu, et al., "Ultra-wide band channel calculation by SBR/Image techniques for indoor communication," *Journal of Electromagnetic Waves and Applications*, Vol. 20, 41–54, 2006.
10. Wan, J. X., C. H. Liang, and J. Lei, "A fast analysis of scattering from microstrip antennas over a wide band," *Progress In Electromagnetics Research*, PIER 50, 187–208, 2005.
11. Das, S., A. Chakrabarty, and A. Chakraborty, "Characteristics of an offset longitudinal/transverse slot coupled crossed waveguide junction using multiple cavity modeling technique considering the T_{e00} mode at the slot aperture," *Progress In Electromagnetics Research*, PIER 67, 297–316, 2007.
12. Wang, F. J. and J. S. Zhang, "Wideband cavity-backed patch antenna for PCS/IMT2000/2.4 Ghz WLAN," *Progress In Electromagnetics Research*, PIER 74, 39–46, 2007.